Developmental Cell
Article

The BAR Domain Protein Arfaptin-1 Controls Secretory Granule Biogenesis at the *trans*-Golgi Network

Helmuth Gehart,[1,2] Alexander Goginashvili,[1,2] Rainer Beck,[3] Joëlle Morvan,[1] Eric Erbs,[1] Ivan Formentini,[2] Maria Antonietta De Matteis,[4] Yannick Schwab,[1] Felix T. Wieland,[3] and Romeo Ricci[1,2,5,*]
[1]Institut de Génétique et de Biologie Moléculaire et Cellulaire (IGBMC), INSERM, CNRS, Université de Strasbourg, 67404 Illkirch, France
[2]Institute of Cell Biology, ETH Zürich, 8093 Zürich, Switzerland
[3]Heidelberg University Biochemistry Center, Heidelberg University, 69120 Heidelberg, Germany
[4]Telethon Institute of Genetics and Medicine, 80131 Napoli, Italy
[5]Nouvel Hôpital Civil, Laboratoire de Biochimie et de Biologie Moléculaire, Université de Strasbourg, 67091 Strasbourg, France
*Correspondence: romeo.ricci@igbmc.fr
http://dx.doi.org/10.1016/j.devcel.2012.07.019

SUMMARY

BAR domains can prevent membrane fission through their ability to shield necks of budding vesicles from fission-inducing factors. However, the physiological role of this inhibitory function and its regulation is unknown. Here we identify a checkpoint involving the BAR-domain-containing protein Arfaptin-1 that controls biogenesis of secretory granules at the *trans*-Golgi network (TGN). We demonstrate that protein kinase D (PKD) phosphorylates Arfaptin-1 at serine 132, which disrupts the ability of Arfaptin-1 to inhibit the activity of ADP ribosylation factor, an important component of the vesicle scission machinery. The physiological significance of this regulatory mechanism is evidenced by loss of glucose-stimulated insulin secretion due to granule scission defects in pancreatic β cells expressing nonphosphorylatable Arfaptin-1. Accordingly, depletion of Arfaptin-1 leads to the generation of small nonfunctional secretory granules. Hence, PKD-mediated Arfaptin-1 phosphorylation is necessary to ensure biogenesis of functional transport carriers at the TGN in regulated secretion.

INTRODUCTION

Sorting and packaging of cargo, proper coating of vesicles and their subsequent detachment from the *trans*-Golgi network (TGN) require complex and dynamic mechanisms (Kirchhausen, 2000). These are particularly important in specialized secretory cells in which big amounts of cargo are transported in vesicles from the TGN to the plasma membrane for subsequent release. Regulated secretion of insulin from pancreatic β cells constitutes one important example as its lack in mammals is incompatible with life and its dysfunction leads to diabetes (Muoio and Newgard, 2008). While most attention has been drawn to distal steps of insulin exocytosis, i.e., vesicle fusion with the plasma membrane (Eliasson et al., 2008), mechanisms underlying correct formation of the secretory granule are still poorly elucidated. Recently, we described the requirement of protein kinase D 1 (PKD1) in pancreatic β cells to control TGN function and insulin secretion (Sumara et al., 2009). Several subsequent studies corroborated the importance of PKD1 in insulin release (Kong et al., 2010; Saini et al., 2010; Subathra et al., 2011).

PKD1, together with PKD2 and PKD3 belong to the protein kinase D (PKD) family of serine/threonine protein kinases of the calcium/calmodulin-dependent kinase group (Rozengurt et al., 2005). Among other important cellular functions (Fu and Rubin, 2011; Rykx et al., 2003), PKD was suggested to control fission of surface-destined cargo-containing vesicles from the TGN (Liljedahl et al., 2001). PKD has been shown to regulate lipid-modifying effectors at the TGN (Fugmann et al., 2007; Hausser et al., 2005; Ngo and Ridgway, 2009), which may impact on membrane dynamics and thus vesicle formation as well as secretion (Malhotra and Campelo, 2011). By binding to diacylglycerol (DAG), PKD is recruited to TGN membranes (Baron and Malhotra, 2002) where it can associate with ADP-ribosylation factor 1 (ARF1) (Pusapati et al., 2010). ARFs are members of the Ras superfamily of small GTPases and are involved both in vesicle budding (Kirchhausen, 2000; Spang, 2008) and vesicle fission (Beck et al., 2011; Pucadyil and Schmid, 2009; Valente et al., 2012) at the TGN. Class I ARFs (ARF1 and ARF3) and Class II ARFs (ARF4 and ARF5) localize to the Golgi compartment, whereas class III ARFs (ARF6) localize to the plasma membrane (Gillingham and Munro, 2007). In addition to these three classes, there are over 20 ARF-like (ARL) proteins in the ARF protein family. Although the GDP-GTP switch of ARF family members is well studied (Donaldson and Jackson, 2011), the mechanisms that direct ARFs to their site of action and govern their interaction with their multiple downstream effectors are poorly understood.

One group of potential ARF regulators is the Arfaptin family consisting of Arfaptin-1, Arfaptin-2, protein kinase C-binding protein 1 (PICK1), and islet cell antigen 69 kDa (ICA69) (Habermann, 2004). Two of its members, Arfaptin-1 and 2, have been shown to interact with ARF1, ARF3, ARF5, ARF6, and ARL1 (Kanoh et al., 1997; Man et al., 2011; Shin and Exton, 2001). The defining feature of Arfaptins is the crescent Bin/amphiphysin/Rvs (BAR)

domain. BAR-domain-containing proteins are key players in membrane dynamics as their crescent shape allows them to impose or sense curvature on lipid bilayers (McMahon and Gallop, 2005). Recent in vitro studies have shown opposing roles of amphipathic helices and BAR domains in membrane fission (Boucrot et al., 2012; Mim et al., 2012). Crescent BAR domains stabilize tubular membrane structures and limit the access of proteins with amphipathic helices, which are sufficient to induce fission. However, the physiological relevance of the inhibition of fission by BAR domains and mechanisms of its regulation have not been elucidated thus far.

Here we show that secretory granule biogenesis at the Golgi requires the BAR domain protein Arfaptin-1 and its regulation by PKD to prevent premature fission and generation of nonfunctional transport carriers. In addition, we demonstrate that Arfaptin-1 is pivotal for maintaining insulin secretion from pancreatic β cells, highlighting the physiological relevance of this mechanism.

RESULTS

PKD Phosphorylates Arfaptin-1 In Vitro and In Vivo

To address a potential functional link between PKD and ARFs, we screened ARFs and known direct interactors of ARFs for PKD consensus phosphorylation motifs (LXRXXpS) and crossreferenced the hits with a recent phosphoproteomic study (Huttlin et al., 2010). Arfaptin-1 displayed a single PKD consensus site, which was phosphorylated in several analyzed tissues (Huttlin et al., 2010). This potential PKD phosphorylation site is present in both the long and short Arfaptin-1 isoform, which differ by 32 amino acids in the N-terminal region. The candidate serine is located at position 132 in the long and at position 100 in the short isoform. This site is highly conserved in vertebrates but is absent in the Arfaptin-1 paralog Arfaptin-2 (Figure 1A).

To prove that Arfaptin-1 is a direct target of PKD, we performed an in vitro kinase assay. Full-length recombinant human Arfaptin-1 was strongly phosphorylated by recombinant active PKD1 (Figure 1B). Addition of the PKD inhibitor Gö6976 (Haxhinasto and Bishop, 2003) abrogated phosphorylation of wild-type Arfaptin-1. Replacement of serine 132 by alanine (Arfaptin-1 S132A) led to complete loss of the phosphorylation signal (Figure 1B). In order to address Arfaptin-1 phosphorylation in cells, we raised a monoclonal antibody against phosphorylated Arfaptin-1, that recognized only phosphorylated wild-type Arfaptin-1 and did not reveal a signal for Arfaptin-1 S132A (Figure 1C). Cells expressing both Flag-tagged wild-type Arfaptin-1 and green fluorescent protein (GFP)-tagged wild-type PKD1 showed strong phosphorylation of exogenous Arfaptin-1 (Figure 1D). Cells coexpressing wild-type Arfaptin-1 and GFP alone showed weak but detectable basal phosphorylation, most likely due to basal activity of endogenous PKD1. Coexpression of wild-type Arfaptin-1 with a GFP-tagged K618N kinase-dead mutant of PKD1 (PKD1 KD-GFP) decreased the signal below basal phosphorylation levels. This is in line with the fact that PKD1 KD acts in a dominant-negative fashion (Liljedahl et al., 2001). Phosphorylation was abolished when Arfaptin-1 S132A was coexpressed either with GFP, wild-type PKD1 or PKD1 KD-GFP. Phosphorylation of endogenous Arfaptin-1 was not detectable in this experiment. Abundance of endogenous or exogenous Arfaptin-1 was not affected upon expression of wild-type and PKD1 KD-GFP. To substantiate dependence of Arfaptin-1 phosphorylation on PKD1 activity, we generated stable knockdowns of PKD1 and corresponding nonsilencing control cells and expressed Flag-tagged wild-type Arfaptin-1. In nonsilencing cells, kinase activity-dependent autophosphorylation of PKD1 was strongly induced by phorbol myristate acetate (PMA), a known activator of PKD1 (Valverde et al., 1994) (Figure 1E). Activation and abundance of PKD1 was strongly reduced for both independent PKD1 knockdowns. Phosphorylation of exogenous Arfaptin-1 was only detected in stimulated cells and was markedly reduced in cells with a knockdown of PKD1 (Figure 1E). In conclusion, these data demonstrate that PKD1 phosphorylates Arfaptin-1 at serine 132 in vitro and in vivo.

Phosphorylation at Serine 132 Delocalizes Arfaptin-1 from the Golgi

To study the functional role of Arfaptin-1 phosphorylation, we examined the effects of PKD1 activity on subcellular localization of Arfaptin-1 and Arfaptin-2. Arfaptin-1 and 2 colocalized with the Golgi protein Giantin in nontransfected cells (Figures S1A and S1B available online), which is in line with recently reported Golgi localization of these two proteins (Man et al., 2011). Expression of GFP alone did not affect localization of Arfaptin-1 and 2. In contrast, in cells expressing PKD1-GFP, most Arfaptin-1 delocalized from the Golgi (Figure 2A), while Arfaptin-2 localization was not affected. Expression of a GFP-tagged constitutively active form of PKD1, in which two activatory serines in the activation loop (serine 744 and 748) have been replaced by glutamic acids (PKD1 2S2E-GFP), led to the same effects (Figure 2A). However, expression of PKD1 KD-GFP did not lead to delocalization of Arfaptin-1 or 2 from the Golgi (Figure 2A) corroborating the requirement of PKD1 kinase activity for controlling Arfaptin-1 localization.

We next investigated whether PKD1-dependent phosphorylation of Arfaptin-1 is required for its change in localization. We coexpressed wild-type PKD1 or PKD1 KD-GFP with Flag-tagged wild-type or Arfaptin-1 S132A. Expression of wild-type PKD1 led to delocalization of wild-type Arfaptin-1 from the Golgi, while expression of PKD1 KD-GFP had no effect (Figure S1C). In strong contrast, Arfaptin-1 S132A remained at the Golgi even when PKD1 was coexpressed, indicating that serine 132 phosphorylation is required for the change in localization of Arfaptin-1 (Figure S1C).

We next addressed whether serine 132 phosphorylation is sufficient to induce Arfaptin-1 delocalization from the Golgi. We expressed GFP-tagged wild-type Arfaptin-1, Arfaptin-1 S132A, and a phosphomimetic mutant of Arfaptin-1 in which serine 132 is replaced with an aspartate (Arfaptin-1 S132D). Wild-type Arfaptin-1 was mainly localized at the Golgi. However, a minor cytoplasmic distribution was detected (Figure 2B), while Arfaptin-1 S132A was more strictly confined to the Golgi apparatus with significantly less detectable cytoplasmic localization. In strong contrast, Arfaptin-1 S132D was diffusely distributed throughout the cytoplasm with minimal retention on Golgi structures (Figure 2B). These results suggest that Arfaptin-1 phosphorylation at serine 132 is required and sufficient to induce its change in localization.

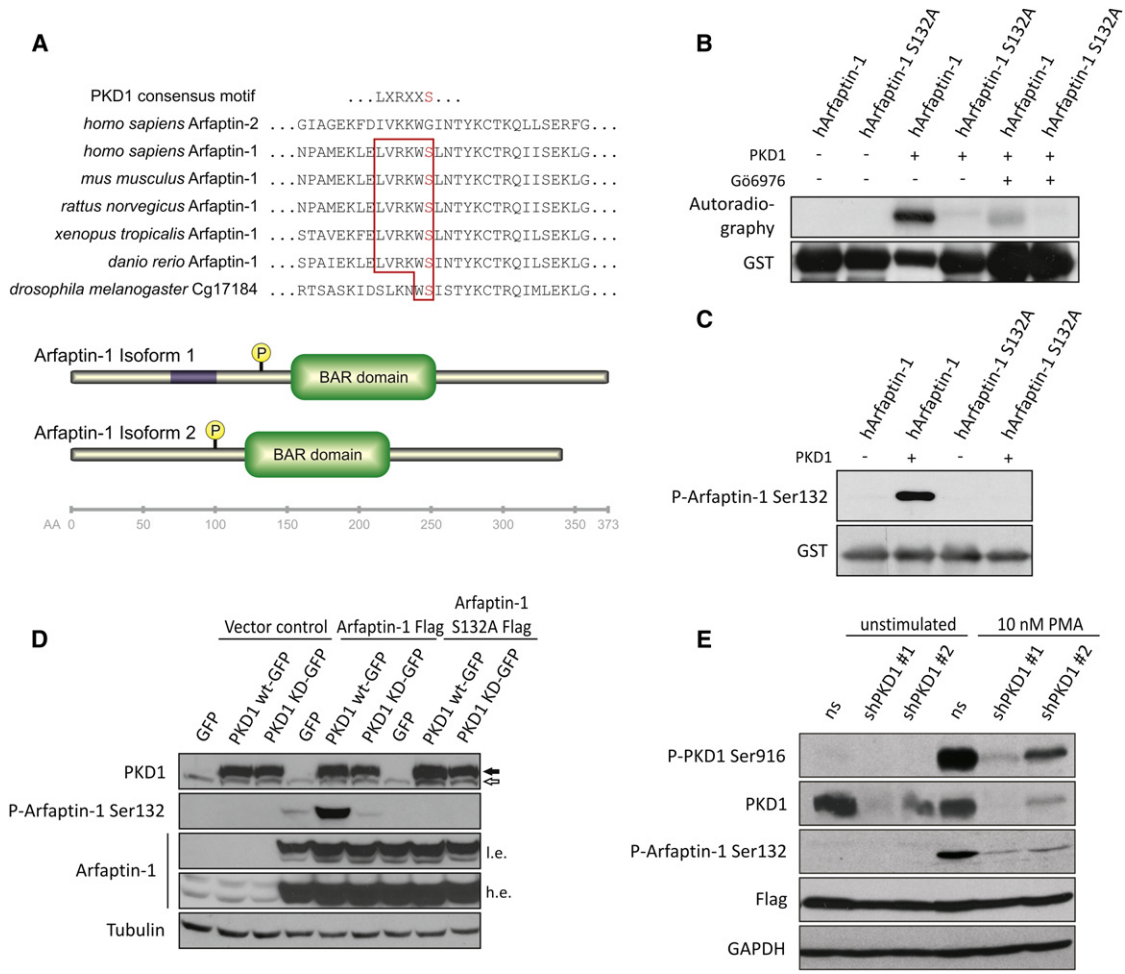

Figure 1. PKD Phosphorylates Arfaptin-1 at Serine 132

(A) Protein sequence alignment of human Arfaptin-2 and Arfaptin-1 as well as of Arfaptin-1 in indicated species. The phosphorylation site is highlighted in red and its position within the full-length protein is indicated below. The region in blue is only present in the longer isoform 1.

(B) In vitro kinase assay using recombinant GST-tagged wild-type human Arfaptin-1 (hArfaptin-1) and serine to alanine mutant Arfaptin-1 (hArfaptin-1 S132A) after addition of recombinant PKD1 without or with the PKD inhibitor Gö6976.

(C) Recombinant wild-type Arfaptin-1 and Arfaptin-1 S132A incubated with or without recombinant PKD1 were blotted using monoclonal antibodies against phosphorylated serine 132 of Arfaptin-1 (P-Arfaptin-1 Ser132). Anti-GST was used as loading control.

(D) Whole-cell lysates of HEK293T cells expressing indicated PKD1 and Arfaptin-1 constructs were blotted for PKD1, phospho-Arfaptin-1 Ser132 and Arfaptin-1. Anti-tubulin was used as loading control. The filled arrow indicates exogenous PKD1, the open arrow endogenous PKD1. l.e., low exposure; h.e., high exposure. Both endogenous Arfaptin-1 isoforms can be detected in cells expressing Flag control in the higher exposure panel.

(E) Whole-cell lysates of HEK293T cells infected with lentiviruses containing two independent shRNA against PKD1 (shPKD1#1 and shPKD1#2) or nonsilencing shRNA and transiently transfected with Arfaptin-1 Flag were blotted using antibodies against autoactivatory phosphorylation of serine 916 of PKD1 (P-PKD1 Ser916), PKD1, P-Arfaptin-1 Ser132 and Flag. Anti-GAPDH was used as loading control. Cells were stimulated with 10 nM phorbol myristate acetate (PMA) for 15 min where indicated.

Phosphorylation at Serine 132 Releases Arfaptin-1-Mediated Inhibition of ARF Activity and Allows Vesicle Formation at the Golgi In Vitro

Given the proximity of serine 132 to the BAR domain, we next addressed whether phosphorylation influences its functions. Since Arfaptins need to dimerize to establish the crescent shaped BAR domains (Tarricone et al., 2001) we tested if dimerization is affected by phosphorylation. Incubation of recombinant glutathione S-transferase (GST)-tagged wild-type Arfaptin-1, Arfaptin-1 S132A, or Arfaptin-1 S132D with lysates from cells that overexpressed Flag-tagged wild-type Arfaptin-1 and subsequent GST pull-downs showed that Arfaptin-1 phosphorylation at serine 132 does not influence the protein's ability to form homodimers (Figure S2A). Using deletion mutants, Williger et al. identified two regions in Arfaptin-1 that are necessary for ARF3 binding (Williger et al., 1999). Since one of them contains serine 132, we examined changes in ARF binding. GST pull-downs were performed with recombinant wild-type Arfaptin-1, Arfaptin-1 S132A, or Arfaptin-1 S132D in presence or absence of guanosine 5′-O-[gamma-thio]triphosphate (GTPγS) with lysates from cells expressing ARF1-HA, ARL1-Myc, or ARF3-HA. ARFs and ARL1 coprecipitated with wild-type

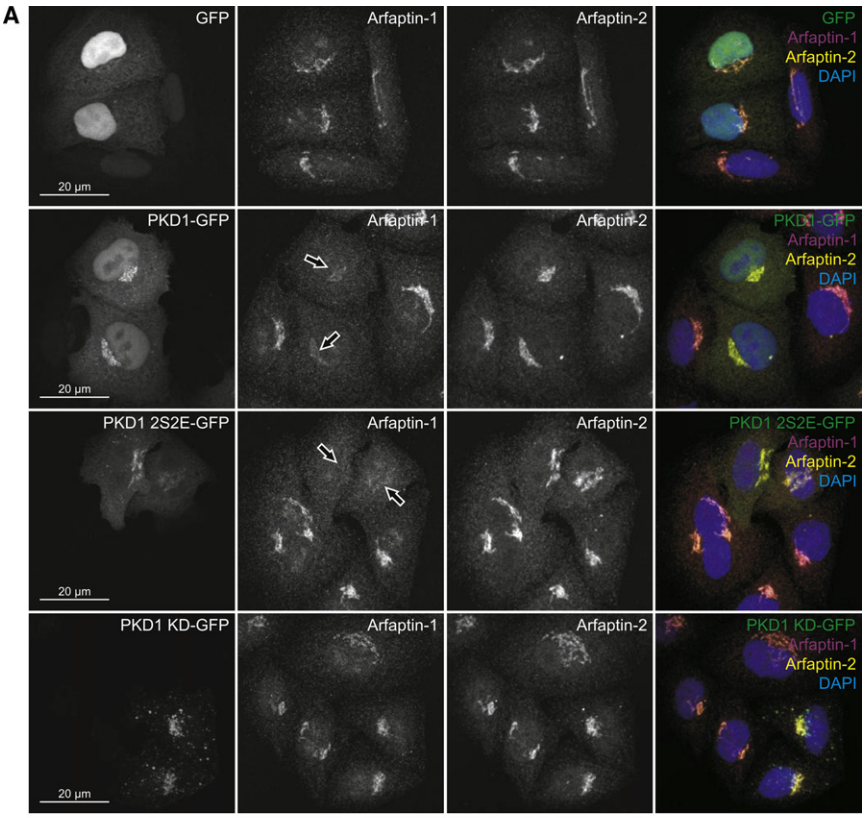

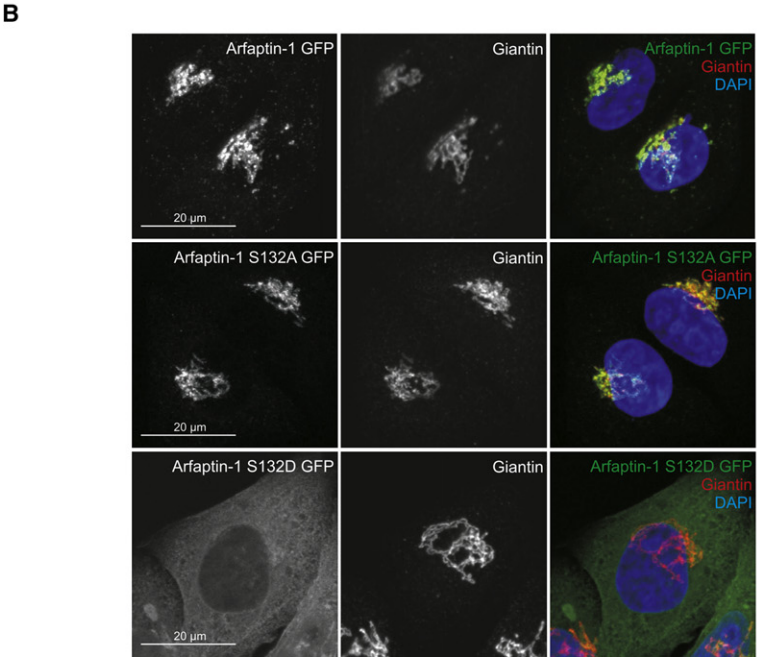

Figure 2. Phosphorylation of Arfaptin-1 at Serine 132 Delocalizes It from the Golgi

(A) Confocal images of HeLa cells expressing GFP, PKD1-GFP, PKD1 2S2E-GFP, or PKD1 KD-GFP. Endogenous Arfaptin-1 and Arfaptin-2 were stained by immunofluorescence and nuclei with DAPI. Arrows indicate reduction of Golgi-localized Arfaptin-1.

(B) Confocal images of HeLa cells transiently expressing GFP-tagged wild-type Arfaptin-1 (Arfaptin-1 GFP), GFP-tagged serine to alanine mutant (Arfaptin-1 S132A-GFP) or GFP-tagged serine to aspartate mutant Arfaptin-1 (Arfaptin-1 S132D-GFP). Giantin staining was used to highlight the Golgi.

See also Figure S1.

Arfaptin-1 and Arfaptin-1 S132A only in the presence of GTPγS (Figures 3A and 3B; Figure S2B), confirming previously reported specificity of Arfaptin-1 for the active (GTP-bound) form of these small GTPases (Kanoh et al., 1997). Strikingly, however, Arfaptin-1 S132D did not interact with ARFs or ARL1 (Figures 3A and 3B; Figure S2B). Likewise, Flag-tagged wild-type Arfaptin-1 or Arfaptin-1 S132A coimmunoprecipitated HA-tagged constitutive active ARF1 (ARF1 Q71L) and endogenous ARL1, while Arfaptin-1 S132D did not (Figures 3C and 3D). Importantly, binding to Arfaptin-1 S132A was markedly higher than binding to wild-type Arfaptin-1 as phosphorylation of the latter was likely to occur in cells due to endogenous PKD activity. To corroborate these findings, we also performed GST pull-downs with unphosphorylated and PKD1-phosphorylated wild-type Arfaptin-1 with lysates from cells expressing ARF1-HA, confirming data obtained with mutant Arfaptin-1 (Figure S2C). We thus conclude that PKD1-mediated phosphorylation of Arfaptin-1 prevents its binding to ARF and ARF-like family members. As binding to ARF family members is required for Golgi localization of Arfaptin-1 (Kanoh et al., 1997; Man et al., 2011), this finding is in line with the change in Arfaptin-1 localization that is observed upon its phosphorylation by PKD1.

We subsequently addressed whether Arfaptin-1 shields activated ARFs or ARF-like proteins from interacting with their downstream effectors. Recently, it has been reported that ARL1 binds and recruits BIG1 and BIG2, guanine nucleotide exchange factors (GEFs) of ARF1 and 3, to the TGN (Christis and Munro, 2012). Interestingly, recruitment of BIG was inhibited by ectopic expression of Arfaptin-1 due to steric hindrance of the interaction of ARL1 with BIG. We thus asked whether phosphorylation at serine 132 abolishes this effect. In GFP-expressing cells, BIG2 localized to the Golgi. In cells expressing GFP-tagged wild-type Arfaptin-1 or Arfaptin-1 S132A, however, localization of BIG2 at the Golgi was dramatically reduced (Figure 3E). In contrast,

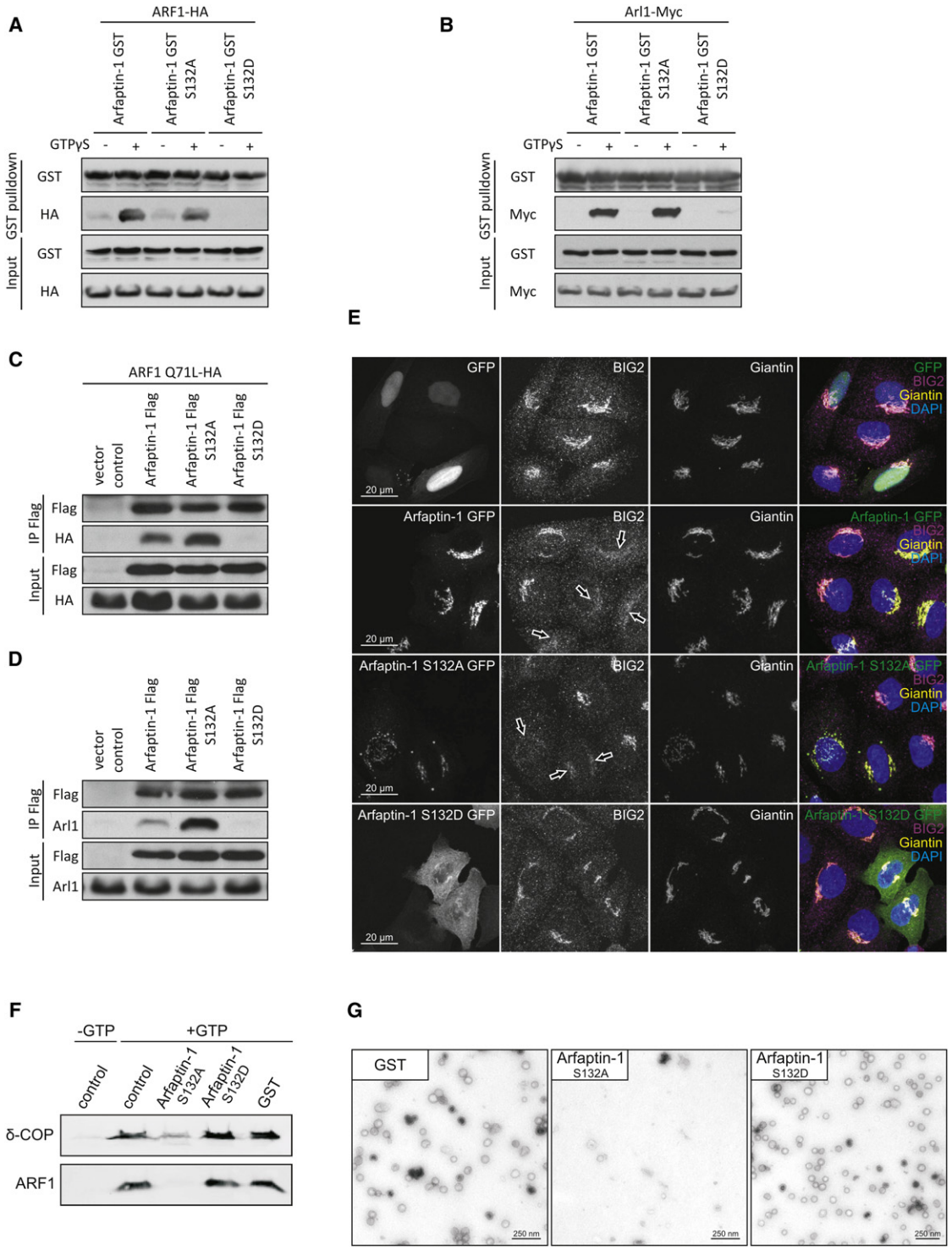

Figure 3. Phosphorylation of Arfaptin-1 at Serine 132 Disrupts Its Interaction with ARF Family Members and Releases Their Inhibition

(A) Western blot after GST pull-down from lysates of HEK293T lysates expressing hemagglutinin (HA)-tagged ADP ribosylation factor 1 (ARF1-HA) incubated with recombinant wild-type Arfaptin-1 (Arfaptin-1 GST), serine to alanine mutant Arfaptin-1 (Arfaptin-1 GST S132A), or serine to aspartate mutant Arfaptin-1 (Arfaptin-1 GST S132D). Antibodies against GST and HA were used to detect proteins with respective tags. GTPγS was added where indicated to lock the small GTPases in their active conformation. GST pull-down and input are shown as indicated.

(B) Western blot after GST pull-down from lysates of HEK293T lysates expressing Myc-tagged ARF-like 1 (ARL1-Myc) incubated with recombinant wild-type Arfaptin-1 GST, Arfaptin-1 GST S132A, or Arfaptin-1 GST S132D. Antibodies against GST and Myc were used to detect proteins with respective tags. GTPγS was added where indicated to lock the small GTPases in their active conformation. GST pull-down and input are shown as indicated.

expression of Arfaptin-1 S132D had no effect on BIG2 localization. Our data thus confirm that binding of active ARL1 by Arfaptin-1 inhibits its interaction with BIG2 and demonstrate that this mechanism is dependent on the phosphorylation status of Arfaptin-1. PKD1 may thus act to derepress Arfaptin-1-imposed inhibition of ARFs, ARF-like proteins and their effectors. This mechanism thus adds another level of ARF regulation beyond classical GTPase cycling.

ARFs contain amphipathic helices that can make shallow insertions into membranes. ARFs were shown to promote membrane fission in their GTP-bound form. In an in vitro reconstitution assay, Beck et al. have shown that ARF1 dimerization is necessary for vesicle fission (Beck et al., 2011). Using the same assay, we investigated whether the phosphorylation status of Arfaptin-1 influences the ability of ARF1 to generate vesicles from purified Golgi. Addition of Arfaptin-1 S132D did not affect vesicle formation as seen both by western blotting (Figure 3F) and electron microscopy (Figure 3G) of the purified vesicle fraction. However, addition of Arfaptin-1 S132A almost completely abolished vesicle generation in vitro (Figures 3F and 3G). These data thus suggest that Arfaptin-1 blocks ARF activity and Golgi vesicle formation in its unphosphorylated state, but allows transport carrier generation to occur upon its phosphorylation and release from ARF proteins.

Phosphorylation of Arfaptin-1 by PKD and Delocalization of Arfaptin-1 Occur in Insulin-Secreting Cells

Recently, we discovered that PKD1 controls TGN dynamics in β cells to regulate insulin secretion and glucose homeostasis in mice (Sumara et al., 2009). We thus asked whether PKD1-mediated phosphorylation of Arfaptin-1 occurs in insulin-secreting cells in response to a physiologic stimulus. To this end, we performed immunoprecipitations of endogenous phosphorylated Arfaptin-1 in a rat insulinoma-derived β cell line (INS-1) after stimulation with the insulin secretagogue carbachol, an acetylcholine analog and known activator of PKD1 (Sumara et al., 2009). In unstimulated cells, Arfaptin-1 phosphorylation was below the detection limit (Figure 4A). Carbachol stimulation, however, induced phosphorylation of Arfaptin-1, which was abolished when PKD1 was inhibited with Gö6976 (Figure 4A). We next analyzed whether carbachol stimulation affected endogenous Arfaptin-1 localization in INS-1 cells. In unstimulated INS-1 cells, Arfaptin-1 was localized at the Golgi and to a lesser extent in the cytoplasm (Figure 4B). Stimulation by carbachol led to a significant decrease of Arfaptin-1 signal at the Golgi. Incubation with the PKD inhibitor Gö6976 decreased carbachol-induced Arfaptin-1 delocalization (Figures 4B and 4C). Thus, physiologic stimulation of PKD activity induces phosphorylation and delocalization of endogenous Arfaptin-1 in β cells.

Nonphosphorylatable Arfaptin-1 Interferes with Glucose-Stimulated Insulin Secretion by Blocking Insulin Granule Fission at the Golgi

ARF activity has been shown to be crucial in regulated secretion (Béglé et al., 2009; Sadakata et al., 2010). As shown above, PKD1-dependent phosphorylation of Arfaptin-1 regulates its interaction with ARF and ARF-like proteins and Golgi vesicle formation in vitro. We thus asked whether PKD-mediated Arfaptin-1 phosphorylation regulates insulin granule formation at the TGN, thereby having impact on insulin secretion.

To answer this question, we investigated short- and long-term effects of pharmacological inhibition of PKD on glucose-stimulated insulin secretion (GSIS). Since Gö6976 was toxic for INS-1 cells for incubations longer than 8 hr, we used CID 755673, a more specific, cell-active PKD inhibitor of the newest generation (Sharlow et al., 2008). CID 755673 efficiently reduced carbachol-stimulated PKD1 activation in INS-1 cells already after 30 min of inhibitor treatment (Figure 5A). In spite of efficient PKD inhibition, no significant reduction in GSIS was measurable 1 hr after inhibitor treatment (Figure 5B). Thus, PKD activity is very unlikely to affect fusion of readily releasable insulin granules that have been generated prior inhibition. After 8 hr of inhibitor treatment, however, stimulated insulin release was significantly reduced. After 24 hr of inhibitor treatment, GSIS was almost completely abolished (Figure 5B). The time frame of the secretion block by PKD inhibition suggests failures in generation and replenishment of functional secretory granules and corroborates a defect at the Golgi level.

To examine whether nonphosphorylatable Arfaptin-1 can mimic the effect of PKD inhibition, we expressed GFP-tagged wild-type Arfaptin-1, Arfaptin-1 S132A, and Arfaptin-1 S132D in INS-1 cells (Figure S3A). Expression of wild-type protein caused a significant decrease in GSIS. Strikingly, Arfaptin-1 S132A almost entirely blocked stimulated insulin release, while Arfaptin-1 S132D had no significant effect on GSIS (Figure 5C). From these results, we conclude that ectopic expression of wild-type Arfaptin-1 shifted the balance between Arfaptin-1-mediated ARF inhibition and PKD1-dependent derepression of the latter, resulting in a moderate loss of GSIS. The S132A mutant, however, was no longer released from binding to ARFs and ARF-like proteins by PKD1 causing a significantly stronger

(C) Anti-Flag immunoprecipitation from lysates of HEK293T cells coexpressing HA-tagged constitutive active ARF1 (ARF1 Q71L) and Flag-tagged wild-type Arfaptin-1, Arfaptin-1 S132A, or Arfaptin-1 S132D. Antibodies against HA and Flag were used to detect proteins with respective tags. Flag immunoprecipitation and input are shown as indicated.
(D) Anti-Flag immunoprecipitation from lysates of HEK293T cells expressing Flag-tagged wild-type Arfaptin-1, Arfaptin-1 S132A, or Arfaptin-1 S132D. Antibodies against ARL1 and Anti-Flag were used to detect endogenous ARL1 and tagged proteins. Flag immunoprecipitation and input are shown as indicated.
(E) Confocal images of cells expressing GFP, GFP-tagged wild-type Arfaptin1 (Arfaptin1-GFP), serine to alanine mutant Arfaptin1 (Arfaptin1 S132A-GFP), or serine to aspartate mutant Arfaptin1 (Arfip1 S132D-GFP). Cells were stained for BIG2, Giantin and DAPI was used to stain the nuclei. Arrows indicate the reduction of Golgi-localized BIG2.
(F and G) Vesicles were reconstituted from isolated Golgi membranes using ARF1 in the presence of GTPγS, purified coatomer and recombinant GST or GST-tagged recombinant Arfaptin-1 mutant protein as indicated. The vesicle fraction was separated from Golgi membranes via sucrose density centrifugation.
(F) Western blot of the purified vesicle fraction of the ARF1 vesicle reconstitution assay. The amount of generated vesicles was measured by quantifying the amounts of δ-COP and ARF1 after vesicle purification. (G) Negative staining electron microscopy of vesicles generated in the ARF1 vesicle reconstitution assay. See also Figure S2.

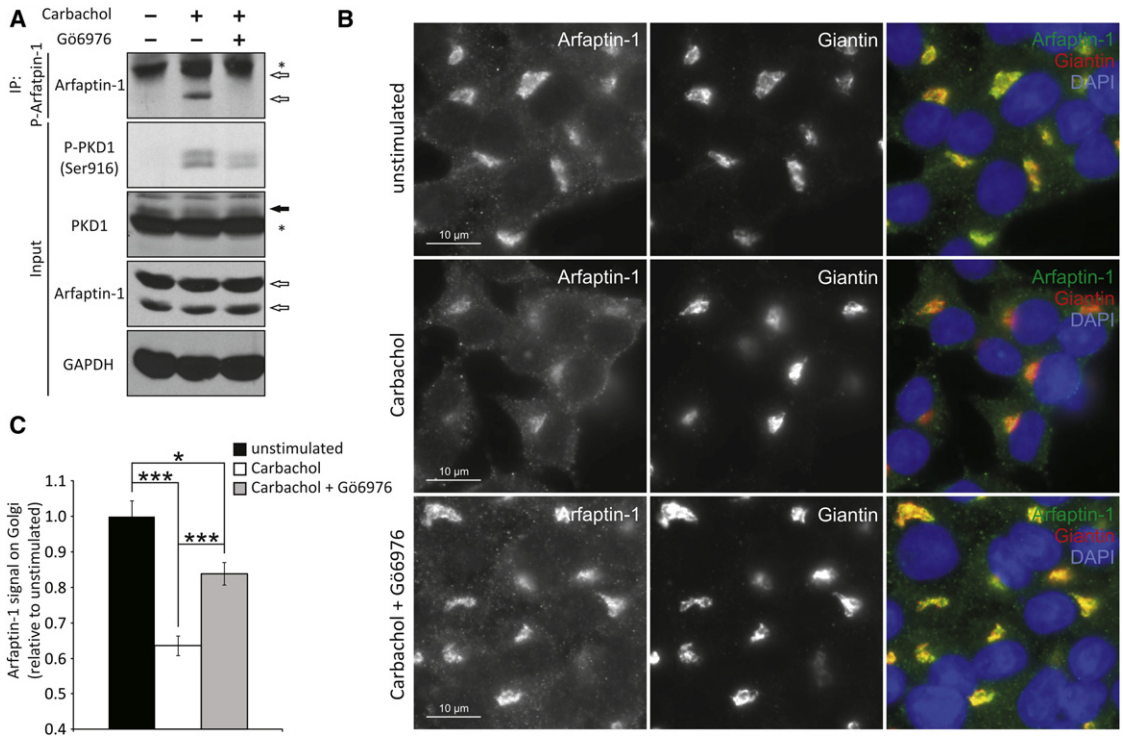

Figure 4. PKD Phosphorylates Arfaptin-1 in Insulin-Secreting Cells upon a Physiologic PKD Stimulus

(A) Immunoprecipitation of phosphorylated Arfaptin-1 (P-Arfaptin-1) from lysates of INS-1 cells stimulated for 15 min with 100 μM carbachol where indicated in presence or absence of the PKD inhibitor Gö6976. Antibodies against Arfaptin-1, autoactivatory phosphorylation of serine 916 of PKD1 (P-PKD1 Ser916), PKD1, and GAPDH (loading control) were used to detect respective proteins. Open arrows point to Arfaptin-1-specific bands. The filled arrow indicates PKD1. * indicates unspecific bands.

(B) Immunofluorescence of INS-1 cells stimulated for 15 min with 100 μM carbachol in presence or absence of the PKD inhibitor Gö6976. Cells were stained for Arfaptin-1 and Giantin. DAPI was used to stain nuclei.

(C) Quantification of relative Arfaptin-1 to Giantin signal intensity on Golgi (n = 10). ns, nonsignificant. *$p < 0.05$; **$p < 0.01$; ***$p < 0.001$ (Student's t test). Error bars indicate mean ± SEM.

inhibitory effect. The S132D mutant does not bind to ARFs or ARF-like proteins and is mostly cytoplasmic. Hence, binding of endogenous Arfaptin-1 to ARFs or ARF-like proteins and its regulation by PKD1 was unimpeded resulting in normal secretion.

Subsequently, we addressed whether Arfaptin-1 overexpression also interferes with constitutive secretion. To this end, we cotransfected a thermosensitive VSV-G mutant (Presley et al., 1997) with Arfaptin-1 Flag, Arfaptin-1 S132A Flag, Arfaptin-1 S132D Flag, or Flag control into INS-1 cells. No differences in VSV-G trafficking were detected (Figure S3B), indicating that expression of Arfaptin-1 or its mutants does not affect constitutive secretion. These results were confirmed using secreted embryonic alkaline phosphatase (SEAP) (Figure S3C). Hence, expression of Arfaptin-1 or Arfaptin-1 S132A interferes with regulated secretion, but does not alter constitutive secretion in β cells.

Given strong inhibition of ARF1-mediated vesicle formation by Arfaptin-1 S132A in vitro and the striking effects on GSIS in vivo, we subsequently explored if the nonphosphorylatable mutant interferes with granule biogenesis. We thus proceeded to investigate insulin granule morphology and distribution using electron microscopy. While there was no significant change in total cellular granule numbers (see Table S1), the distribution of granules throughout the cell was severely altered in cells expressing Arfaptin-1 S132A as compared to controls. The number of granules close to the plasma membrane was significantly reduced, while the number of granules in the Golgi compartment or the surrounding cytoplasm was more than doubled (Figure 5D; Figures S3D and S3E). Most strikingly, Arfaptin-1 S132A-expressing cells revealed many neck-shaped membrane structures connecting insulin granules with each other or with the Golgi apparatus (Figure 5E). Such structures were almost not detectable in control cells (Figure 5F). Both the increased number of necks and prevalence of unsuccessfully separated granule structures point to a severe defect in membrane scission. Interestingly, the phenotype was associated with a slightly reduced total insulin content (Figure S3A). Conclusively, nonphosphorylatable Arfaptin-1 limits fission of insulin transport carriers and replenishment of functional secretory granules.

Arfaptin-1-Imposed Inhibition of Membrane Fission at the Golgi Serves as a Checkpoint for Proper Insulin Granule Formation

Lack of Arfaptin-1 phosphorylation interferes with ARF function, insulin granule biogenesis and insulin secretion. However, an

important question remained. What happens to insulin secretion if negative regulation of ARF activity by Arfaptin-1 is lost in cells? To answer this question, we established a stable knockdown of Arfaptin-1 in INS-1 cells (Figure S4A). Strikingly, depletion of Arfaptin-1 almost completely abolished insulin secretion in response to glucose (Figure 6A). Furthermore, there was no additional effect of PKD inhibition with CID 755673 on GSIS in Arfaptin-1-depleted INS-1 cells underscoring the importance of Arfaptin-1 as a target of PKD (Figure S4B). No differences in VSV-G trafficking were detectable in Arfaptin-1 depleted as compared to control cells (Figure S4C), indicating that loss of Arfaptin-1 does not affect constitutive secretion. These results were confirmed using SEAP (Figure S4D) corroborating a specific function of Arfaptin-1 in regulated but not constitutive secretion.

Since our experiments implicated Arfaptin-1 in granule scission, we analyzed granule morphology and distribution using quantitative transmission electron microscopy (TEM). Comparison of the total number of insulin granules in Arfaptin-1 knockdown and control cells did not show any significant differences (Table S1). However, the size of secretory granules in INS-1 cells depleted of Arfaptin-1 was markedly reduced (Figures 6B and 6C). Moreover, in control cells the majority of granules were found in proximity of the plasma membrane. These vesicles constitute the reserve pool of secretory granules (Rorsman et al., 2000). In INS-1 cells depleted of Arfaptin-1, however, the number of granules close to the plasma membrane was markedly reduced (Figure 6D). Likewise, the amount of granules primed for insulin release and docked with the plasma membrane—the readily releasable pool—was strongly diminished (Figure 6E). Instead, secretory granules of Arfaptin-1 knockdown cells were found distributed throughout the cytoplasm indicating their inability to reach the plasma membrane (Figure 6F).

Since defective insulin granule biogenesis is likely to affect packaging of insulin into transport carriers, we analyzed both proinsulin and insulin levels in control and Arfaptin-1 knockdown cells. Both proinsulin and insulin levels were strongly reduced in cells lacking Arfaptin-1 (Figure 6G). To exclude that the latter was a result of decreased proinsulin production, we performed pulse-chase experiments with radioactively labeled S^{35}-methionine. After 30 min of label incorporation both control and Arfaptin-1 knockdown cells showed comparable proinsulin levels indicating that preproinsulin transcription, translation and conversion to proinsulin occurs normally in Arfaptin-1 depleted cells (Figure 6H). After 3 hr of chase the proinsulin signal in control cells was no longer detectable, since proinsulin had been successfully converted into insulin. In Arfaptin-1 knockdown cells, the proinsulin band was gone as well; however, only a very weak band for mature insulin was detectable (Figure 6H). Thus, the pulse-chase experiment did not show a delay or defect in insulin conversion in Arfaptin-1-deficient cells. Instead, the data indicate that a significant portion of labeled hormone had not been stored in functional secretory granules and was most likely rapidly degraded. These results provide strong evidence that Arfaptin-1 is necessary for correct formation of secretory granules and thus stimulated insulin secretion.

Altogether, our data demonstrate that Arfaptin-1 inhibits fission of insulin granules prior its phosphorylation by PKD to prevent formation of nonfunctional transport carriers in insulin-secreting β cells.

DISCUSSION

Recently, the mechanisms how BAR-domain-containing proteins regulate membrane fission have been uncovered (Boucrot et al., 2012; Mim et al., 2012). Our study demonstrates how the activity of one of them, Arfaptin-1, is regulated to ensure proper secretory granule formation at the Golgi of pancreatic β cells.

The BAR domain of Arfaptin-1 is known to sense highly positive membrane curvatures (Habermann, 2004; Peter et al., 2004). The highest membrane curvature at the Golgi is found at the neck of a growing vesicle. Arfaptin-1 has thus a tropism for the vesicle neck (Habermann, 2004), and has the potential to stabilize it by forming a scaffold that prevents membrane fission (Boucrot et al., 2012; Mim et al., 2012). Shedding of such a scaffold would not only physically destabilize the vesicle neck, but would subsequently allow access for the scission complex. Thus, as long as Arfaptin-1 is bound to activated ARF at the vesicle neck, ARF is shielded from interaction with downstream effectors and fission is prevented (Figure 7A). Once PKD phosphorylates Arfaptin-1 at serine 132, it is released from ARF and fission inhibition is relieved (Figure 7B). The actual machinery that accomplishes fission of secretory granules is unknown so far. One interesting possibility is that scission is mediated directly by ARF dimers, which have the ability to fission membranes through their N-terminal amphipathic helices (Beck et al., 2011). A similar mechanism has been reported for another ARF family member, Sar1, and the fission of Coat Protein (COP) II-coated vesicles (Bielli et al., 2005). Alternatively, ARF may recruit a fission machinery (Figure 7C), as it has been shown that PKD and ARF are components of a protein complex involved in carrier scission at the TGN (Valente et al., 2012).

We show that PKD phosphorylates Arfaptin-1 at serine 132, a modification that disrupts its binding to small GTPases of the ARF family. Although the region including serine 132 has been reported to be important for ARF binding (Williger et al., 1999), it is not clear at this point how this phosphorylation event interferes with ARF binding. So far two structures of Arfaptin in complex with small GTPases have been resolved (Nakamura et al., 2012; Tarricone et al., 2001). Crystallization experiments in both studies were performed with N-terminally truncated Arfaptin that does not contain serine 132. Nevertheless, the structure of dimerized Arfaptin bound to two ARL1 molecules published by Nakamura et al. (2012) demonstrated that binding to ARF and binding to positively curved membranes (Habermann, 2004; Peter et al., 2004) are not mutually exclusive as they involve different interaction surfaces of the protein. It is likely that both interactions work cooperatively to recruit Arfaptin-1 to the neck of forming secretory granules.

Interestingly, our data show that Arfaptin-1 is necessary for regulated but not constitutive secretion. Our results thus indicate that control of membrane fission might be distinct for both secretory pathways. The generation of transport carriers in both secretory pathways requires ARFs. However, secretory granules and constitutively secreted vesicles strongly differ in

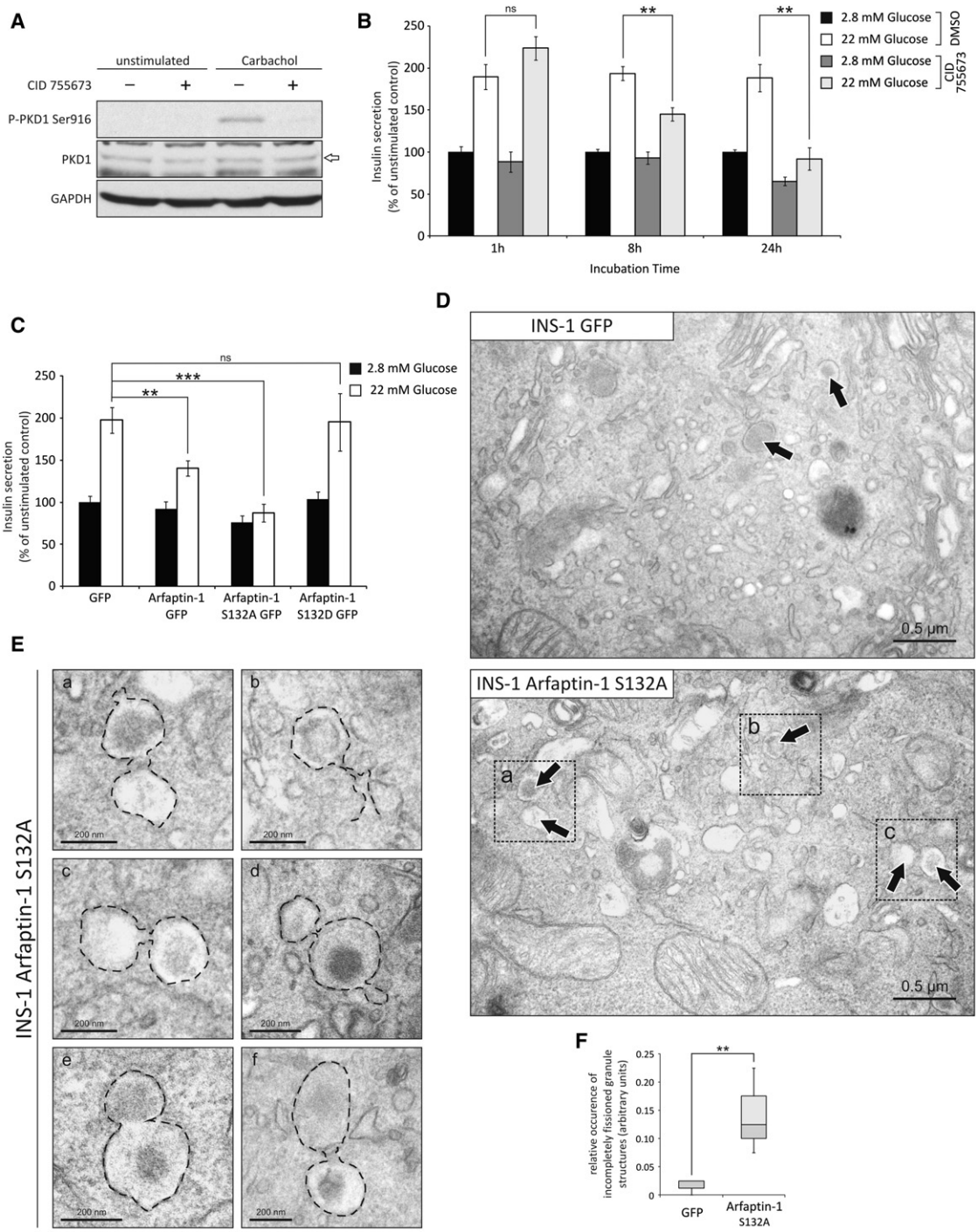

Figure 5. PKD-Mediated Arfaptin-1 Phosphorylation Is Specifically Required for Insulin Granule Scission and Thereby Glucose-Stimulated Insulin Secretion

(A) INS-1 cells were preincubated for 15 min with CID 755673 or DMSO control and subsequently stimulated for 15 min with 20 μM carbachol in the presence of DMSO or CID 755673. Whole-cell lysates were blotted for P-PKD1 Ser916, PKD1, and GAPDH as loading control.

(B) Insulin secretion at basal (2.8 mM) and stimulatory (22 mM) glucose concentrations from INS-1 cells treated with DMSO or 30 μM PKD inhibitor CID 755673 for the indicated time period (n = 6).

(C) Insulin secretion from INS-1 cells stably expressing GFP, GFP-tagged wild-type Arfaptin-1, serine to alanine mutant Arfaptin-1 (Arfaptin-1 S132A-GFP) or serine to aspartate mutant Arfaptin-1 (Arfaptin-1 S132D-GFP) under basal (2.8 mM) and stimulatory (22 mM) glucose concentrations (GFP n = 6, Arfaptin-1 GFP n = 6, Arfaptin-1 S132A-GFP n = 6, Arfaptin-1 S132D-GFP n = 9).

(D) Representative transmission electron microscopy images of the Golgi area in GFP-expressing control and GFP-tagged Arfaptin-1 S132A-overexpressing INS-1 cells. Arrows indicate secretory granules.

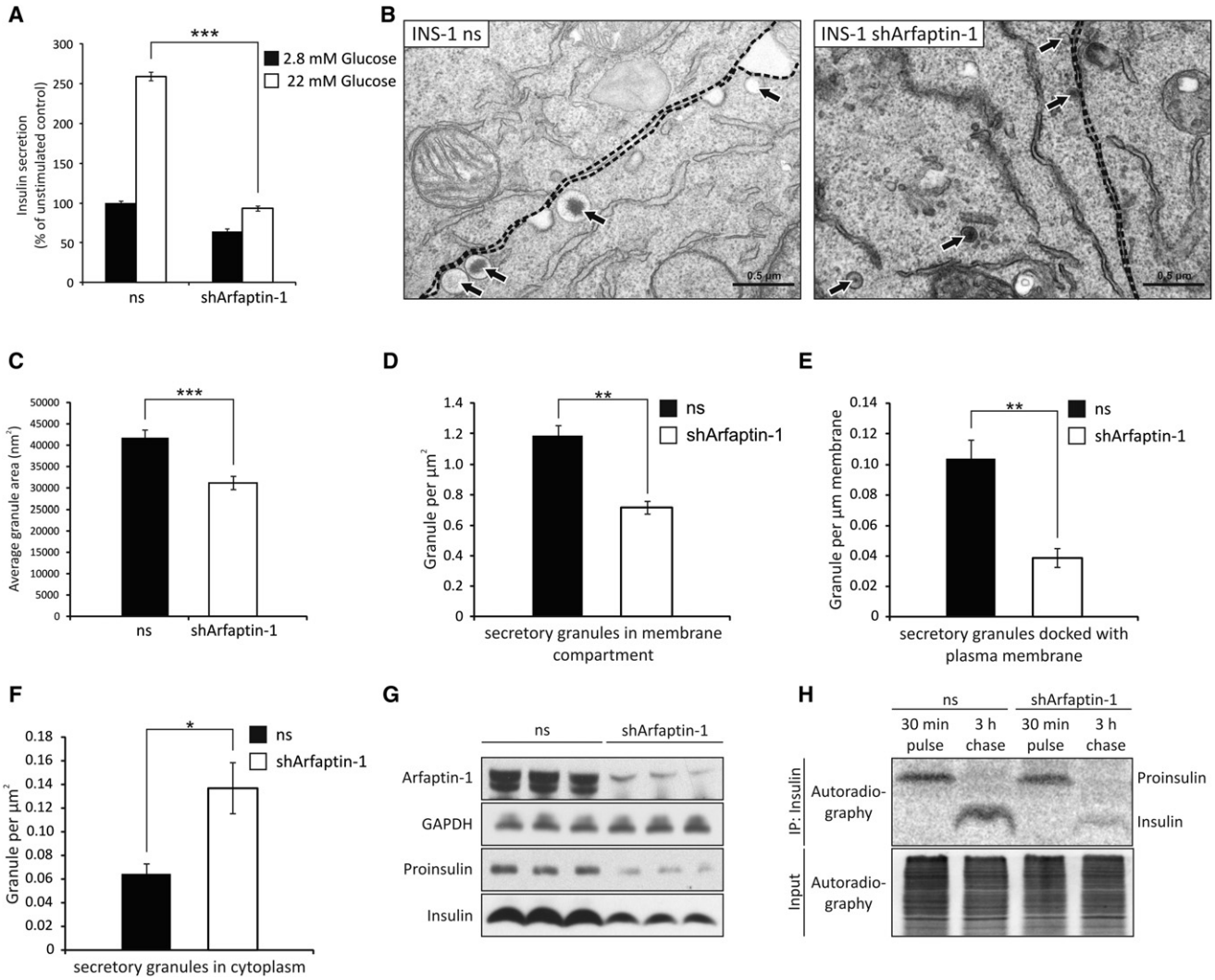

Figure 6. Arfaptin-1 Is Necessary for Proper Insulin Granule Formation

(A) Insulin secretion from INS-1 cells infected with control nonsilencing (ns) or Arfaptin-1 knockdown (shArfaptin-1) constructs under basal (2.8 mM) and stimulatory (22 mM) glucose concentrations (n = 6).

(B) Representative transmission electron microscopy images of nonsilencing (ns) control and Arfaptin-1 knockdown (shArfaptin-1) INS-1 cells. Arrows indicate secretory granules. Dashed lines show the plasma membrane.

(C) Mean granule size of secretory granules in nonsilencing control or Arfaptin-1 knockdown INS-1 cells (n = 200).

(D) Quantification of the number of secretory granules in vicinity of the plasma membrane (n = 30).

(E) Quantification of the number of secretory granules docked to the plasma membrane (n = 30).

(F) Quantification of the number of secretory granules in the cytoplasm (n = 30).

(G) Total cell lysates of ns and shArfaptin-1 INS-1 cells separated on a Tricine gel. Antibodies against Proinsulin, Insulin and GAPDH (loading control) were used to detect the respective proteins.

(H) Autoradiography of immunoprecipitated insulin after 30 min of S^{35} methionine incubation (pulse) and 3 hr of chase with nonradioactive medium (chase) in control and Arfaptin-1 knockdown INS-1 cells. Autoradiography of total cell lysates before immunoprecipitation is shown as input.

In (A) and (C)–(F), *p < 0.05, **p < 0.01, ***p < 0.001 (Student's t test). Error bars indicate mean ± SEM. See also Figure S4.

size. The specificity of Arfaptin-1 for secretory granules may thus be due to its BAR domain that has a tropism for vesicle necks of a specific size.

We demonstrate that the release of Arfaptin-1 by PKD phosphorylation is necessary for the formation of functional granules in insulin-secreting cells. Both overexpression of

(E) Magnifications of abnormal insulin granules in Arfaptin-1 S132A-overexpressing cells. The dashed line indicates the granule membrane.

(F) Box plot of relative occurrence of unseparated granule structures in GFP control and Arfaptin-1 S132A-overexpressing cells. Whiskers indicate minimum and maximum values. Significance was calculated using Yates' Chi-square test (n = 30).

In (B) and (C), ns, nonsignificant; *p < 0.05, **p < 0.01, ***p < 0.001 (Student's t test). Error bars indicate mean ± SEM. See also Figure S3.

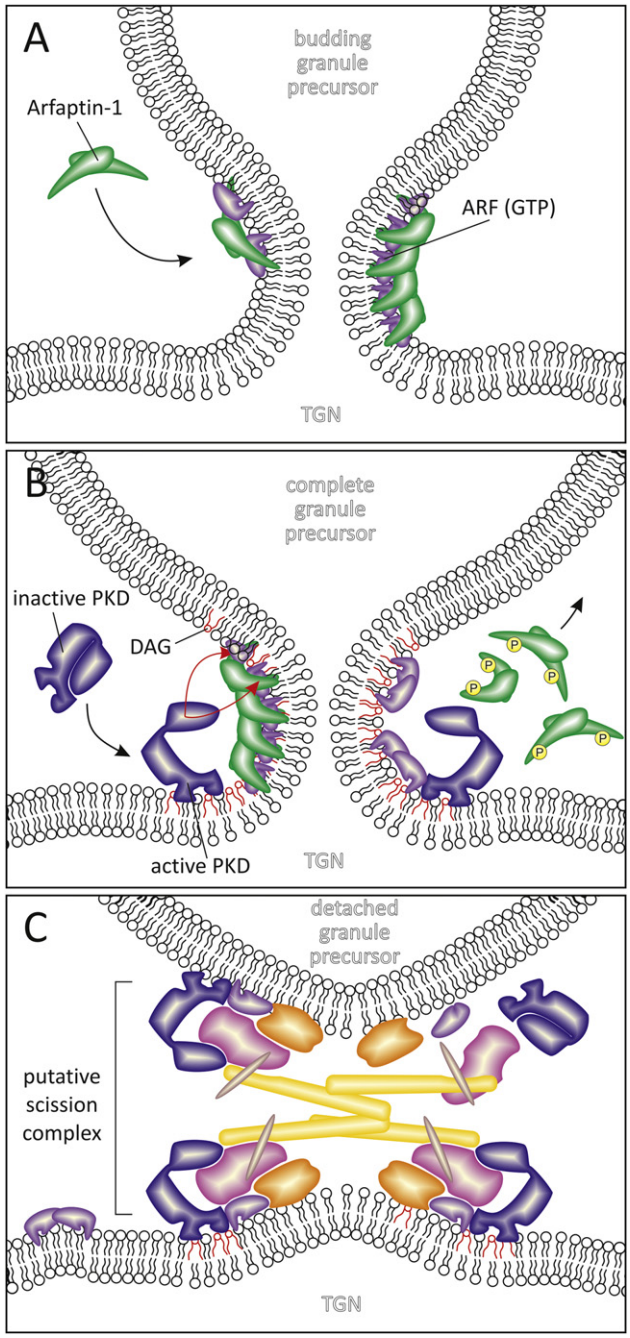

Figure 7. Model of the Secretory Granule Scission Checkpoint

(A) Arfaptin-1 binds ARF-GTP at the neck of a growing secretory granule precursor and forms a protective scaffold. As long as Arfaptin-1 is bound to an ARF family member, the latter is shielded from interacting with downstream effectors and cannot dimerize.

(B) Once the granule precursor has been completely loaded, its increased size induces strong curvature at the vesicle neck, priming it for local diacylglycerol (DAG, indicated as red lipids) accumulation. DAG is a strong activator of PKD and recruits the kinase by binding to the C1a and C1b domain. Active PKD phosphorylates Arfaptin-1 at serine 132 and releases it from ARFs.

(C) ARFs that are no longer shielded by Arfaptin-1 induce fission via their amphipathic helices after dimerization or nucleate together with PKD a scission complex. Finally, the scission machinery detaches the secretory granule precursor from the TGN.

a nonphosphorylatable Arfaptin-1 mutant and pharmacological inhibition of PKD activity interfere with insulin secretion in response to glucose. Remarkably, pharmacological inhibition of PKD does not block secretion immediately. This observation suggests that granules that have been formed before PKD inhibition can still be secreted. However, secretory defects upon PKD inhibition become apparent at later time points, where replenishment of newly formed functional granules is essential to maintain secretion. This observation is also corroborated by the presence of nonfunctional granules and obvious fission defects in Arfaptin-1 S132A-overexpressing cells. Interestingly, the fission defect in these cells resulted in incompletely separated granules of normal size, which may imply the existence of an upper granule size limit. However, it is unknown so far whether an unidentified vesicle coat or different size sensing mechanisms limit the granule size.

Loss-of-function experiments also strongly support a role of Arfaptin-1 in generation of functional insulin granules as secretory granules in Arfaptin-1 knockdown cells are small and nonfunctional. Additionally, our pulse-chase experiments show that a significant portion of newly synthesized proinsulin in cells depleted of Arfaptin-1 is rapidly degraded instead of being properly stored in functional secretory granules. This conclusion is further supported by decreased total insulin and proinsulin levels in Arfaptin-1 knockdown cells. Interestingly, granule numbers in Arfaptin-1 knockdown and control cells were comparable. Degradation of improperly formed granules may thus counteract increased granule generation due to premature fission finally resulting in comparable numbers of granules, which are small, nonfunctional and contain less insulin. This phenotype can be explained by the absence of a checkpoint that halts vesicle fission until all necessary components have been sorted into the forming granule. We suggest that Arfaptin-1 and PKD are at the core of this checkpoint and ensure that only properly formed secretory granules can detach from the Golgi.

How PKD senses that a granule precursor is ready for release from the TGN is still unclear. However, diacylglycerol (DAG), a phospholipid known to be a strong activator of PKCs and PKD, is enriched in membranes with high negative curvature due to its small hydrophilic head and bulky hydrophobic tail (Szule et al., 2002). Therefore, increasing curvature and accumulation of DAG in the growing vesicle's neck could account for local PKD activation once the granule reaches a certain size.

A small perturbation in the process of granule formation can blunt a β cell's secretory capacity, as only a limited amount of granules can be primed for release at a certain time (20 granules per β cell; Eliasson et al., 2008). Thus, if this readily releasable pool of vesicles is clogged up by a subpopulation of defective granules, even correctly formed ones could no longer release their cargo. Therefore, generation of defective transport carriers could account for the commonly observed first- and second-phase insulin secretion defects in patients suffering from type II diabetes (Del Prato et al., 2002).

Altogether, our work uncovers a quality control mechanism of transport carrier formation at the TGN that ensures continuous replenishment of functional secretory granules. This mechanism is pivotal in insulin-secreting cells and may thus be key in maintaining glucose homeostasis and energy metabolism.

EXPERIMENTAL PROCEDURES

Detailed experimental procedures are available in Supplemental Experimental Procedures.

Glucose-Stimulated Insulin Secretion

GSIS was performed as previously described (Sumara et al., 2009). In brief, INS-1 cells were starved for 30 min in Krebs-Ringer Bicarbonate Buffer (KRB) (136 mM NaCl, 4.7 mM KCl, 1.2 mM $MgS0_4$, 1 mM $CaCl_2$, 1.2 mM KH_2PO_4, 5 mM $NaHCO_3$, 10 mM HEPES [pH 7.4]) supplemented with 0.5% BSA, and 2.8 mM glucose. Subsequently, INS-1 cells were incubated for 1 hr in the same buffer. The cellular supernatant was taken off as unstimulated sample, and replaced by KRB supplemented with 0.5% BSA and 22 mM glucose. After 1 hr the supernatant was taken off as stimulated sample and the remaining cells were lysed in IP Buffer. The insulin secretion in the supernatants was measured using an Ultra Sensitive Mouse Insulin ELISA Kit (Christal Chem Inc.). Data were normalized to nonstimulated control cells. To measure insulin secretion in INS-1 cells expressing exogenous Arfaptin-1, cells were lentivirally transfected with GFP fusion constructs 72 hr before the secretion experiments.

ARF1 Vesicle Reconstitution Assay

One hundred twenty-five micrograms of salt-washed Golgi membranes (Beck et al., 2009) was mixed with 5 μg myristoylated ARF1, 40 μg coatomer, 45 μg Arfaptin-1 mutants or 15 μg free GST, and 1 mM GTP in assay buffer (25 mM HEPES-KOH [pH 7], 2.5 mM Mg-Acetate, 100 mM DTT) in a total volume of 250 μl. After incubation for 10 min at 37°C, the salt concentration was raised to 250 mM KCl and the sample was centrifuged at 12,000 × *g* for 10 min. The supernatant containing COPI vesicles was loaded on top of two sucrose cushions (5 μl of 50% and 50 μl of 37% sucrose) and centrifuged for 50 min at 100,000 × *g* in a SW60Ti rotor. COPI-coated vesicles were concentrated at the interphase between 50% and 37% sucrose. Fifty percent of the isolated vesicle fraction was analyzed by SDS-PAGE and western blotting. For negative staining electron microscopy a carbon coated grid was put on top of a 5 μl droplet of purified COPI vesicles. After 10 min of adsorption at room temperature proteins were fixed by putting the grid onto a 20 μl droplet of 1% glutaraldehyde in 1 × assay buffer (25 mM HEPES-KOH [pH 7], 2.5 mM MgAcetate), washed three times with 20 μl assay buffer each and incubated for 5 min in 0.05% of tannic acid. All these steps were performed at room temperature. Afterward, the sample was washed four times with 20 μl water. Then staining was performed with 0.4% uranyl acetate in 1.8% methylcellulose for 10 min on ice.

Pulse-Chase Insulin Biosynthesis Assay

Proinsulin biosynthesis and conversion of proinsulin to insulin were analyzed by (pro)insulin immunoprecipitation of [^{35}S]methionine-radiolabeled INS-1 lysates as described (Wicksteed et al., 2001). Briefly, INS-1 cells were incubated in KRB with 25 mM glucose for 1 hr, the last 30 min of incubation was carried out in the presence of 250 μCi/ml 35S-methionine (pulse). After pulse, cells were washed and then chased for 0 or 3 hr in KRB buffer with 1.4 mM glucose. At each chase time point, cells were collected, washed, lysed in IP Buffer (50 mM Tris [pH 7.5], 50 mM NaCl, 0.5% Triton X-100, 0.5% NP40 substitute, 5 mM EGTA, 5 mM EDTA, 20 mM NaF, 25 mM beta-glycerophosphate, 1 mM PMSF, 0.1 mM $NaVO_3$, 1 × complete protease inhibitor [Roche]) and subsequently immunoprecipitated for (pro)insulin with anti-insulin antibody (I8510, Sigma). Immunoprecipitated 35S-labeled (pro)insulin was then subjected to SDS-PAGE and visualized by phosphoimager.

VSV-G Constitutive Secretion Assay

The protocol for the VSV-G secretion assay was adapted from Valente et al. (2012). In short, control or Arfaptin-1 knockdown INS-1 cells were transfected with pEGFP-VSVG using the Amaxa Cell Line Nucleofector Kit T (Lonza). Five hours after transfection cells were shifted to 40°C for 30 hr. Subsequently 100 μg/ml cycloheximide was added and the temperature was shifted to 20°C for 30 min. At this point the T0 sample was taken. Cells were shifted to 32°C for 2 hr and the T120 sample was taken and samples were stained without permeabilization with anti-luminal VSVG antibody and DAPI.

SEAP Constitutive Secretion Assay

Control or Arfaptin-1 knockdown INS-1 cells were transfected with pBluescript-CMV-SEAP using the Amaxa Cell Line Nucleofector Kit T (Lonza). SEAP enzymatic activity was measured in lysates and supernatants using Quanti-Blue (Invivogene) according to the manufacturer's instructions.

Statistical Analysis

Pairwise significance was calculated using two-tailed unpaired Student's t test in Microsoft Excel (Microsoft). Data were considered statistically significant once $p < 0.05$. *$p < 0.05$; **$p < 0.01$; ***$p < 0.001$.

SUPPLEMENTAL INFORMATION

Supplemental Information includes four figures, one table, and Supplemental Experimental Procedures and can be found with this article online at http://dx.doi.org/10.1016/j.devcel.2012.07.019.

ACKNOWLEDGMENTS

We thank Vivek Malhotra, CRG Barcelona, for critical scientific inputs. We thank Izabela Sumara for critical reading of the manuscript. This work was supported by the European Foundation for the Study of Diabetes (EFSD, EFSD/GSK Programme Award 2008), by the Swiss Society for Endocrinology and Diabetology (SGED, Young Investigator Award), by an ERC starting grant (ERC-2011-StG, 281271-STRESSMETABOL), and by the Swiss National Science Foundation (SNSF; PP0033-114856). H.G. and A.G. were supported by the EFSD, ERC, and SNSF grants. I.F. was supported by the Bonizzi-Theler Foundation, Zurich. M.A.D.M. acknowledges the support of Telethon and AIRC (AIRC, grant IG 8623).

Received: April 5, 2012
Revised: July 2, 2012
Accepted: July 24, 2012
Published online: September 13, 2012

REFERENCES

Baron, C.L., and Malhotra, V. (2002). Role of diacylglycerol in PKD recruitment to the TGN and protein transport to the plasma membrane. Science *295*, 325–328.

Beck, R., Adolf, F., Weimer, C., Bruegger, B., and Wieland, F.T. (2009). ArfGAP1 activity and COPI vesicle biogenesis. Traffic *10*, 307–315.

Beck, R., Prinz, S., Diestelkötter-Bachert, P., Röhling, S., Adolf, F., Hoehner, K., Welsch, S., Ronchi, P., Brügger, B., Briggs, J.A., and Wieland, F. (2011). Coatomer and dimeric ADP ribosylation factor 1 promote distinct steps in membrane scission. J. Cell Biol. *194*, 765–777.

Béglé, A., Tryoen-Tóth, P., de Barry, J., Bader, M.F., and Vitale, N. (2009). ARF6 regulates the synthesis of fusogenic lipids for calcium-regulated exocytosis in neuroendocrine cells. J. Biol. Chem. *284*, 4836–4845.

Bielli, A., Haney, C.J., Gabreski, G., Watkins, S.C., Bannykh, S.I., and Aridor, M. (2005). Regulation of Sar1 NH2 terminus by GTP binding and hydrolysis promotes membrane deformation to control COPII vesicle fission. J. Cell Biol. *171*, 919–924.

Boucrot, E., Pick, A., Çamdere, G., Liska, N., Evergren, E., McMahon, H.T., and Kozlov, M.M. (2012). Membrane fission is promoted by insertion of amphipathic helices and is restricted by crescent BAR domains. Cell *149*, 124–136.

Christis, C., and Munro, S. (2012). The small G protein Arl1 directs the trans-Golgi-specific targeting of the Arf1 exchange factors BIG1 and BIG2. J. Cell Biol. *196*, 327–335.

Del Prato, S., Marchetti, P., and Bonadonna, R.C. (2002). Phasic insulin release and metabolic regulation in type 2 diabetes. Diabetes *51* (*Suppl 1*), S109–S116.

Donaldson, J.G., and Jackson, C.L. (2011). ARF family G proteins and their regulators: roles in membrane transport, development and disease. Nature Rev. *12*, 362–375.

Eliasson, L., Abdulkader, F., Braun, M., Galvanovskis, J., Hoppa, M.B., and Rorsman, P. (2008). Novel aspects of the molecular mechanisms controlling insulin secretion. J. Physiol. *586*, 3313–3324.

Fu, Y., and Rubin, C.S. (2011). Protein kinase D: coupling extracellular stimuli to the regulation of cell physiology. EMBO Rep. *12*, 785–796.

Fugmann, T., Hausser, A., Schöffler, P., Schmid, S., Pfizenmaier, K., and Olayioye, M.A. (2007). Regulation of secretory transport by protein kinase D-mediated phosphorylation of the ceramide transfer protein. J. Cell Biol. *178*, 15–22.

Gillingham, A.K., and Munro, S. (2007). Identification of a guanine nucleotide exchange factor for Arf3, the yeast orthologue of mammalian Arf6. PLoS ONE *2*, e842.

Habermann, B. (2004). The BAR-domain family of proteins: a case of bending and binding? EMBO Rep. *5*, 250–255.

Hausser, A., Storz, P., Märtens, S., Link, G., Toker, A., and Pfizenmaier, K. (2005). Protein kinase D regulates vesicular transport by phosphorylating and activating phosphatidylinositol-4 kinase IIIbeta at the Golgi complex. Nat. Cell Biol. *7*, 880–886.

Haxhinasto, S.A., and Bishop, G.A. (2003). A novel interaction between protein kinase D and TNF receptor-associated factor molecules regulates B cell receptor-CD40 synergy. J. Immunol. *171*, 4655–4662.

Huttlin, E.L., Jedrychowski, M.P., Elias, J.E., Goswami, T., Rad, R., Beausoleil, S.A., Villén, J., Haas, W., Sowa, M.E., and Gygi, S.P. (2010). A tissue-specific atlas of mouse protein phosphorylation and expression. Cell *143*, 1174–1189.

Kanoh, H., Williger, B.T., and Exton, J.H. (1997). Arfaptin 1, a putative cytosolic target protein of ADP-ribosylation factor, is recruited to Golgi membranes. J. Biol. Chem. *272*, 5421–5429.

Kirchhausen, T. (2000). Three ways to make a vesicle. Nature Rev. *1*, 187–198.

Kong, K.C., Butcher, A.J., McWilliams, P., Jones, D., Wess, J., Hamdan, F.F., Werry, T., Rosethorne, E.M., Charlton, S.J., Munson, S.E., et al. (2010). M3-muscarinic receptor promotes insulin release via receptor phosphorylation/arrestin-dependent activation of protein kinase D1. Proc. Natl. Acad. Sci. USA *107*, 21181–21186.

Liljedahl, M., Maeda, Y., Colanzi, A., Ayala, I., Van Lint, J., and Malhotra, V. (2001). Protein kinase D regulates the fission of cell surface destined transport carriers from the trans-Golgi network. Cell *104*, 409–420.

Malhotra, V., and Campelo, F. (2011). PKD regulates membrane fission to generate TGN to cell surface transport carriers. Cold Spring Harb. Perspect. Biol. *3*, 3.

Man, Z., Kondo, Y., Koga, H., Umino, H., Nakayama, K., and Shin, H.W. (2011). Arfaptins are localized to the trans-Golgi by interaction with Arl1, but not Arfs. J. Biol. Chem. *286*, 11569–11578.

McMahon, H.T., and Gallop, J.L. (2005). Membrane curvature and mechanisms of dynamic cell membrane remodelling. Nature *438*, 590–596.

Mim, C., Cui, H., Gawronski-Salerno, J.A., Frost, A., Lyman, E., Voth, G.A., and Unger, V.M. (2012). Structural basis of membrane bending by the N-BAR protein endophilin. Cell *149*, 137–145.

Muoio, D.M., and Newgard, C.B. (2008). Mechanisms of disease: molecular and metabolic mechanisms of insulin resistance and beta-cell failure in type 2 diabetes. Nature Rev. *9*, 193–205.

Nakamura, K., Man, Z., Xie, Y., Hanai, A., Makyio, H., Kawasaki, M., Kato, R., Shin, H.W., Nakayama, K., and Wakatsuki, S. (2012). Structural basis for membrane binding specificity of the Bin/Amphiphysin/Rvs (BAR) domain of Arfaptin-2 determined by Arl1 GTPase. J. Biol. Chem. *287*, 25478–25489.

Ngo, M., and Ridgway, N.D. (2009). Oxysterol binding protein-related Protein 9 (ORP9) is a cholesterol transfer protein that regulates Golgi structure and function. Mol. Biol. Cell *20*, 1388–1399.

Peter, B.J., Kent, H.M., Mills, I.G., Vallis, Y., Butler, P.J., Evans, P.R., and McMahon, H.T. (2004). BAR domains as sensors of membrane curvature: the amphiphysin BAR structure. Science *303*, 495–499.

Presley, J.F., Cole, N.B., Schroer, T.A., Hirschberg, K., Zaal, K.J., and Lippincott-Schwartz, J. (1997). ER-to-Golgi transport visualized in living cells. Nature *389*, 81–85.

Pucadyil, T.J., and Schmid, S.L. (2009). Conserved functions of membrane active GTPases in coated vesicle formation. Science *325*, 1217–1220.

Pusapati, G.V., Krndija, D., Armacki, M., von Wichert, G., von Blume, J., Malhotra, V., Adler, G., and Seufferlein, T. (2010). Role of the second cysteine-rich domain and Pro275 in protein kinase D2 interaction with ADP-ribosylation factor 1, trans-Golgi network recruitment, and protein transport. Mol. Biol. Cell *21*, 1011–1022.

Rorsman, P., Eliasson, L., Renström, E., Gromada, J., Barg, S., and Göpel, S. (2000). The cell physiology of biphasic insulin secretion. News Physiol. Sci. *15*, 72–77.

Rozengurt, E., Rey, O., and Waldron, R.T. (2005). Protein kinase D signaling. J. Biol. Chem. *280*, 13205–13208.

Rykx, A., De Kimpe, L., Mikhalap, S., Vantus, T., Seufferlein, T., Vandenheede, J.R., and Van Lint, J. (2003). Protein kinase D: a family affair. FEBS Lett. *546*, 81–86.

Sadakata, T., Shinoda, Y., Sekine, Y., Saruta, C., Itakura, M., Takahashi, M., and Furuichi, T. (2010). Interaction of calcium-dependent activator protein for secretion 1 (CAPS1) with the class II ADP-ribosylation factor small GTPases is required for dense-core vesicle trafficking in the trans-Golgi network. J. Biol. Chem. *285*, 38710–38719.

Saini, D.K., Karunarathne, W.K., Angaswamy, N., Saini, D., Cho, J.H., Kalyanaraman, V., and Gautam, N. (2010). Regulation of Golgi structure and secretion by receptor-induced G protein $\beta\gamma$ complex translocation. Proc. Natl. Acad. Sci. USA *107*, 11417–11422.

Sharlow, E.R., Giridhar, K.V., LaValle, C.R., Chen, J., Leimgruber, S., Barrett, R., Bravo-Altamirano, K., Wipf, P., Lazo, J.S., and Wang, Q.J. (2008). Potent and selective disruption of protein kinase D functionality by a benzoxoloazepinolone. J. Biol. Chem. *283*, 33516–33526.

Shin, O.H., and Exton, J.H. (2001). Differential binding of arfaptin 2/POR1 to ADP-ribosylation factors and Rac1. Biochem. Biophys. Res. Commun. *285*, 1267–1273.

Spang, A. (2008). The life cycle of a transport vesicle. Cell. Mol. Life Sci. *65*, 2781–2789.

Subathra, M., Qureshi, A., and Luberto, C. (2011). Sphingomyelin synthases regulate protein trafficking and secretion. PLoS ONE *6*, e23644.

Sumara, G., Formentini, I., Collins, S., Sumara, I., Windak, R., Bodenmiller, B., Ramracheya, R., Caille, D., Jiang, H., Platt, K.A., et al. (2009). Regulation of PKD by the MAPK p38delta in insulin secretion and glucose homeostasis. Cell *136*, 235–248.

Szule, J.A., Fuller, N.L., and Rand, R.P. (2002). The effects of acyl chain length and saturation of diacylglycerols and phosphatidylcholines on membrane monolayer curvature. Biophys. J. *83*, 977–984.

Tarricone, C., Xiao, B., Justin, N., Walker, P.A., Rittinger, K., Gamblin, S.J., and Smerdon, S.J. (2001). The structural basis of Arfaptin-mediated cross-talk between Rac and Arf signalling pathways. Nature *411*, 215–219.

Valente, C., Turacchio, G., Mariggio, S., Pagliuso, A., Gaibisso, R., Di Tullio, G., Santoro, M., Formiggini, F., Spano, S., Piccini, D., et al. (2012). A 14-3-3gamma dimer-based scaffold bridges CtBP1-S/BARS to PI(4)KIIIbeta to regulate post-Golgi carrier formation. Nat. Cell Biol. *14*, 343–354.

Valverde, A.M., Sinnett-Smith, J., Van Lint, J., and Rozengurt, E. (1994). Molecular cloning and characterization of protein kinase D: a target for diacylglycerol and phorbol esters with a distinctive catalytic domain. Proc. Natl. Acad. Sci. USA *91*, 8572–8576.

Wicksteed, B., Herbert, T.P., Alarcon, C., Lingohr, M.K., Moss, L.G., and Rhodes, C.J. (2001). Cooperativity between the preproinsulin mRNA untranslated regions is necessary for glucose-stimulated translation. J. Biol. Chem. *276*, 22553–22558.

Williger, B.T., Provost, J.J., Ho, W.T., Milstine, J., and Exton, J.H. (1999). Arfaptin 1 forms a complex with ADP-ribosylation factor and inhibits phospholipase D. FEBS Lett. *454*, 85–89.